

Ultra-low-noise large-bandwidth transimpedance amplifier

Gino Giusi^{*,†}, Gianluca Cannatà, Graziella Scandurra and Carmine Ciofi

Università degli Studi di Messina (DIECII), Contrada di Dio, I-98166 Messina, Italy

SUMMARY

Equivalent input current noise and bandwidth are the most relevant parameters qualifying a low-noise transimpedance amplifier. In the conventional topology consisting of an operational amplifier in a shunt-shunt configuration, the equivalent input noise decreases as the feedback resistor (R_F), which also sets the gain, increases. Unfortunately, as R_F increases above a few MΩ, as it is required for obtaining high sensitivity, the bandwidth of the system is set by the parasitic capacitance of R_F and reduces as R_F increases. In this paper, we propose a new topology that allows overcoming this limitation by employing a large-bandwidth voltage amplifier together with a proper modified feedback network for compensating the effect of the parasitic capacitance of the feedback resistance. We experimentally demonstrate, on a prototype circuit, that the proposed approach allows to obtain a bandwidth in excess of 100 kHz and an equivalent input noise of about 4 fA/√Hz, corresponding to the current noise of the 1 GΩ resistor that is part of the feedback network. The new approach allows obtaining larger bandwidth with respect to those obtained in previously proposed configurations with comparable background noise. Copyright © 2014 John Wiley & Sons, Ltd.

Received 2 October 2013; Revised 7 June 2014; Accepted 22 July 2014

KEY WORDS: transimpedance amplifier; low-noise amplifier; low-frequency noise; large-bandwidth amplifier

1. INTRODUCTION

Measurement accuracy of low level currents is ultimately limited by the noise introduced by the measurement chain. When dealing with high impedance sources (impedances in the order of tens of MΩ or more), the first stage of the measurement chain is a transimpedance amplifier (TIA), possibly followed by voltage amplifier stages for reaching the desired overall gain. In most cases, the TIA sets the performances of the system in terms of gain, bandwidth and noise floor. When the power of the signal to be measured is much larger than the integrated noise floor of the TIA front-end, the main issue to be addressed in the design is the optimization of the gain-bandwidth trade-off. In many interesting situations, however, the power of the source may be comparable to the TIA noise floor. This is, for example, the case of the measurement of the current fluctuations in electronic devices [1], or currents in single molecular systems and in impedance spectroscopy of molecular biosensors [2, 3]. Current noise measurements have been also used as a powerful tool for gaining detailed insights into the physical mechanisms regulating the charge transport in electron devices [4–7] and for electrical characterization and reliability investigation [8–11]. In all these cases, minimizing the TIA equivalent input noise while maintaining a sufficiently large bandwidth is the most relevant issue to be addressed. This goal is not easily obtained, since, as it will be discussed in the following, a reduction of the equivalent input noise is normally accompanied by a proportional reduction in the useful bandwidth. Indeed, commercial TIAs [12, 13] are capable of reaching equivalent input noise floor in the fA/√Hz order but at the cost of a very limited bandwidth,

*Correspondence to: Gino Giusi, Università degli Studi di Messina (DIECII), Contrada di Dio, I-98166 Messina, Italy.
†E-mail: ggusi@unime.it

typically in the order of hundreds of Hz. When we are interested in the signal spectral density rather than in recording its behavior in the time domain, cross-correlation approaches involving two or more amplifying stages in proper combinations can sometimes be employed in order to obtain very low background noise at the cost of longer measurement times [14–16]. When it is possible to resort to cross-correlation technique, the increase in the intrinsic noise level, resulting from a larger bandwidth, is not, at least in principle, an issue, and therefore larger measurement bandwidths are possible. Note, however, that the averaging time needed to obtain the reduction of the uncorrelated noise down to a given level is proportional to the square of the magnitude of the uncorrelated noise spectra. This means that, even in the cases in which cross correlation can be used, the capability of designing large-bandwidth low-noise TIA is of great importance since it can considerably reduce the measurement time when very low background noise and large bandwidth are required.

The conventional topology of a TIA is made of an operational amplifier (opamp) in a shunt-shunt feedback configuration (Figure 1) where the feedback network consists of a large value resistor R_F . It is the feedback resistance R_F together with its parallel parasitic capacitance C_F , whose value is a weak function of R_F itself for a given resistor technology and circuit layout, that sets both the background noise level and the bandwidth of the system, in such a way as to essentially obtain a constant value for the product between bandwidth and in-bandwidth noise power spectral density. Approaches have been proposed in the literature for compensating the effect of the bandwidth reduction due to C_F for large values of R_F [17, 18]. These approaches essentially reduce to the idea that a second amplifying stage with a proper frequency response can equalize the linear distortion introduced by C_F in the first conventional transimpedance stage. In this paper, we propose a new approach for extending the bandwidth of a TIA that is based on a proper modification of the feedback network for obtaining the equalization of the overall frequency response.

The paper is organized as follows: in Section II, we review the properties of conventional TIAs with focus on modeling, bandwidth and overall equivalent input noise; in Section III, we discuss the new

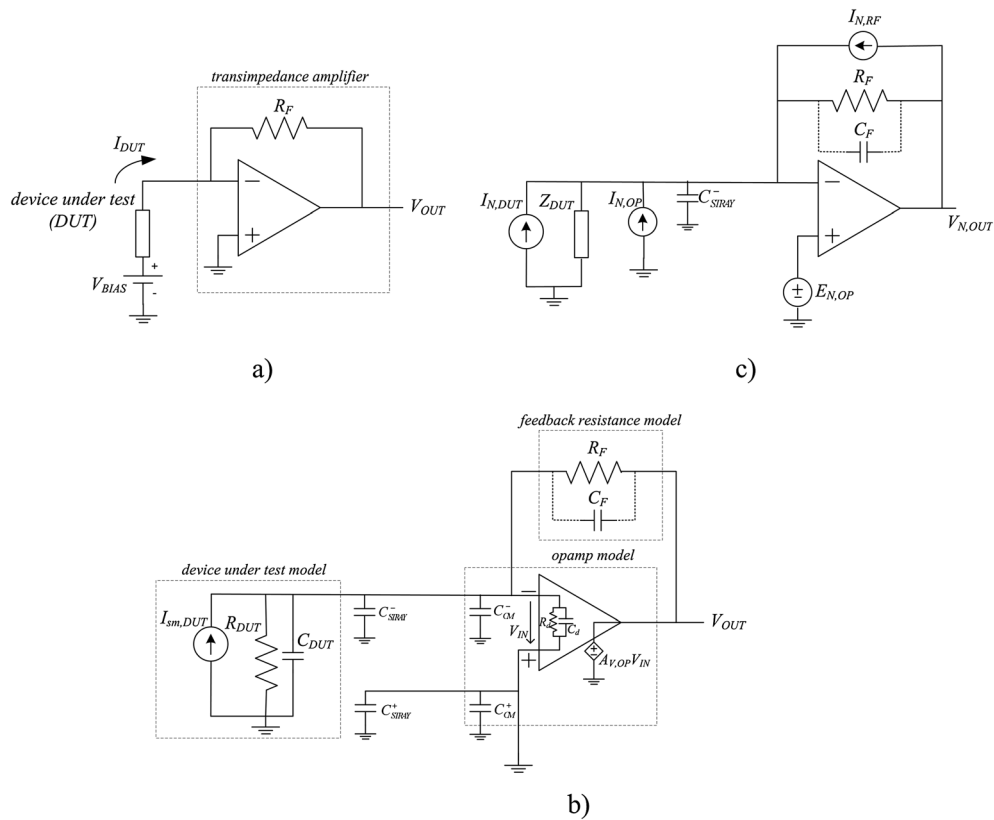


Figure 1. a) Operational amplifier-based implementation of the conventional transimpedance amplifier; b) small signal equivalent circuit; c) equivalent circuit for noise calculation.

approach we propose for increasing the bandwidth of the amplifier without increasing its equivalent input noise; in Section IV, we provide experimental evidence of the validity of the approach we propose; in Section V, we report measured comparison between the proposed TIA and the one reported in [17] and, finally, in Section VI, we draw our conclusions.

2. MODELING, BANDWIDTH AND NOISE ESTIMATION IN CONVENTIONAL TRANSIMPEDANCE AMPLIFIERS

2.1. Modeling of the conventional TIA

A circuital implementation of an operational amplifier (OA)-based conventional TIA is shown in Figure 1a. Under the simplified assumption of virtual short circuit at the inputs of the operational amplifier, the two-terminal device under test (DUT) is biased through the voltage source V_{BIAS} , and the total current through the DUT (I_{DUT}) flows entirely through the feedback resistance R_F , resulting in an output voltage $V_{OUT} = -R_F I_{DUT}$ with a transimpedance gain, with respect to current fluctuations, equal to $-R_F$. For a correct estimation of the system bandwidth, we must take into careful account the parasitic components associated to both the OA and the feedback resistance R_F . In order to discuss the bandwidth of the system, we will refer to the circuit in Figure 1b, representing the small signal equivalent of the circuit in Figure 1a, including all the relevant parasitic components. The DUT is represented by its Norton equivalent, with $I_{N,DUT}$ being the small-signal noise current generated by the DUT itself and Z_{DUT} being the DUT impedance (we assume that the DUT is linear or is linearized around the operating point in Figure 1a) modeled as the parallel of a resistor R_{DUT} and a capacitor C_{DUT} . The OA is modeled by a differential input impedance (Z_d) made of the parallel of a differential input resistance (R_d) and of a differential input capacitance (C_d), by the common mode input capacitances (C_{CM}^- , C_{CM}^+) and by the open-loop voltage gain $A_{V,OP}$ modeled, in turn, as a first-order dominant pole response (DC voltage gain A_{V0} and dominant pole time constant τ_{OP}). The feedback resistor is modeled with its parasitic parallel capacitance C_F . The capacitances C_{STRAY}^+ and C_{STRAY}^- account for layout induced stray capacitive couplings. It is apparent that C_{CM}^+ and C_{STRAY}^+ play no role. In discussing the frequency response and the noise contributions, we will follow the approach of writing down the transfer function $A_S(s)$ from any independent signal or noise source S toward the output V_{OUT} in the form:

$$\begin{aligned} A_S(s) &= \frac{V_{OUT}(s)}{S(s)} = A_S^{VSC}(s)H_L(s) \\ H_L(s) &= \frac{-T(s)}{1 - T(s)} \end{aligned} \quad (1)$$

where $T(s)$ is the loop gain from the input V_{IN} through the operational amplifier and back to the input V_{IN} with all independent sources set to 0 and A_S^{VSC} is the gain calculated in the virtual short circuit approximation, that is assuming $|T(j\omega)| \rightarrow \infty$ and, hence, $H_L(j\omega) = 1$. Note that while A_S^{VSC} depends on the source with respect to which the gain A_S is being calculated, the loop gain is the same for all sources in the circuit.

2.2. Bandwidth Analysis of the conventional TIA

In the Laplace transform domain, the transimpedance gain in the VSC approximation can be readily calculated as

$$A_Z^{VSC}(s) = -Z_F(s) = -\frac{R_F}{1 + sR_F C_F} = -\frac{R_F}{1 + s\tau_F}; \quad \tau_F = R_F C_F \quad (2)$$

while we obtain, for the loop gain $T(s)$:

$$\begin{aligned}
T(s) &= -A_{V,OP}(s) \frac{Z_{IN}(s)}{Z_{IN}(s) + Z_F(s)} \\
A_{V,OP}(s) &= \frac{A_{V0}}{1 + s\tau_{OP}} \quad Z_{IN}(s) = \frac{R_{IN}}{1 + sR_{IN}C_{IN}}
\end{aligned} \tag{3}$$

$$C_{IN} = C_{DUT} + C_{STRAY}^- + C_{CM}^- + C_d \quad R_{IN} = R_{DUT}/R_d$$

that can be rewritten in the form:

$$\begin{aligned}
T(s) &= -\frac{T_0}{1 + s\tau_{OP}} \times \frac{1 + s\tau_F}{1 + \beta_0(1 + \alpha_C)s\tau_F} \\
\alpha_C &= \frac{C_{IN}}{C_F}; \quad \beta_0 = \frac{R_{IN}}{R_{IN} + R_F}; \quad T_0 = \beta_0 A_{V0}
\end{aligned} \tag{4}$$

The term $H_L(s)$ becomes

$$\begin{aligned}
H_L(s) &= \frac{T_0}{1 + T_0} \times \frac{1 + s\tau_F}{as^2 + bs + 1} \approx \frac{1 + s\tau_F}{as^2 + bs + 1} \\
T_0 &>> 1 \quad ; \quad a = \frac{\tau_{OP}\tau_F(1 + \alpha_C)}{A_{V0}} \quad ; \quad b = \frac{\tau_{OP}}{T_0} + \left(\frac{1 + \alpha_C}{A_{V0}} + 1 \right) \tau_F
\end{aligned} \tag{5}$$

and, for the transimpedance gain A_Z :

$$A_Z(s) = -\frac{R_F}{as^2 + bs + 1} \tag{6}$$

The parameter α_C is usually much larger than 1, corresponding to $C_{IN} >> C_F$. Usually, we also have $\tau_{OP} >> \tau_F$. However, because of the very large value of A_{V0} (normally close to 10^6) and T_0 , the following approximations can be made in Equation (5):

$$\frac{1 + \alpha_C}{A_{V0}} << 1; \quad \frac{\tau_{OP}}{T_0} << \tau_F \tag{7}$$

resulting in $b \approx \tau_F$. On the other hand, the coefficient a can be written as:

$$a = \frac{\tau_{OP}\tau_F}{A_{V0}} (1 + \alpha_C) = \frac{\tau_F}{2\pi GBW} (1 + \alpha_C) \tag{8}$$

where GBW is the gain band-width product of the operational amplifier. With these assumptions and positions, the denominator of Equation (6) can be rewritten in the form:

$$\frac{s^2}{\omega_1\omega_2} + \frac{s}{\omega_1} + 1 \tag{9}$$

with:

$$\omega_1 = \frac{1}{\tau_F}; \quad \omega_2 = 2\pi \frac{GBW}{1 + \alpha_C} \tag{10}$$

Note that the angular frequency ω_1 depends on the characteristics of the feedback resistance only, while the angular frequency ω_2 depends on the characteristics of the operational amplifier and on the DUT equivalent capacitance. The poles of the transfer function are:

$$s_{p1} = -\omega_1 \left(\frac{1 + \sqrt{1 - 4 \frac{\omega_1}{\omega_2}}}{2} \right)^{-1} \quad s_{p2} = -\omega_2 \left(\frac{1 + \sqrt{1 - 4 \frac{\omega_1}{\omega_2}}}{2} \right) \quad (11)$$

If $4\omega_1/\omega_2 < < 1$, the bandwidth of the system coincides with $f_F = \omega_1/2\pi$, that is the bandwidth is set by the feedback resistance R_F in combination with its parasitic resistance C_F . This is a typical situation in low-noise measurements for small DUT capacitances. As an example, by means of careful layout design and device selection, the value of C_F can be as low as 0.5 pF with $R_F = 1 \text{ G}\Omega$, corresponding to $f_F \approx 300 \text{ Hz}$; by resorting to a typical OA such as the TLC070, with a GBW of 10 MHz and an input capacitance in the order of 10 pF, the condition $4\omega_1/\omega_2 < < 1$ is certainly satisfied for DUT capacitances lower than 50 pF. However, as the DUT capacitance increases, ω_2 becomes smaller and smaller until complex conjugate poles are obtained when $4\omega_1/\omega_2 > 1$. It is interesting to notice that, if we maintain the definition of the bandwidth as the maximum frequency at which the response is within $\pm 3 \text{ dB}$ with respect to the gain at low frequencies, the bandwidth of the TIA is larger than f_F for $\omega_1/\omega_2 < 1.67$ (Figure 2), reaching a maximum of about $1.3 f_F$ for ω_1/ω_2 close to $1/2$. It is clear, however, that it is the time constant of the feedback resistor that essentially sets the maximum bandwidth that can be obtained in the conventional TIA configuration. If the DUT capacitance increases up to values for which $\omega_1/\omega_2 > > 1$, we obtain a reduction of the bandwidth with respect to the one set by the feedback resistor, coupled with a large peak in the frequency response that may result intolerable in many situations and that can easily lead to instability because of the effect of other singularities (due to both the complete response of the operational amplifier and to the parasitic elements due to the board layout) that have not been included in the previous analysis.

2.3. Noise analysis of the conventional TIA

Figure 1c shows the equivalent circuit of the conventional TIA with all relevant noise sources explicitly shown: $E_{N,OP}$ and $I_{N,OP}$ are the equivalent input voltage and current noise sources of the OA, respectively; $I_{N,DUT}$ is the current noise source of the DUT, and $I_{N,RF}$ is current noise source of the feedback resistance. In order to calculate the power spectrum we assume all noise sources to be uncorrelated, and we will use the expedient of replacing each noise source with fictitious deterministic sources to calculate the frequency response from each source to the output node V_{OUT} . We obtain:

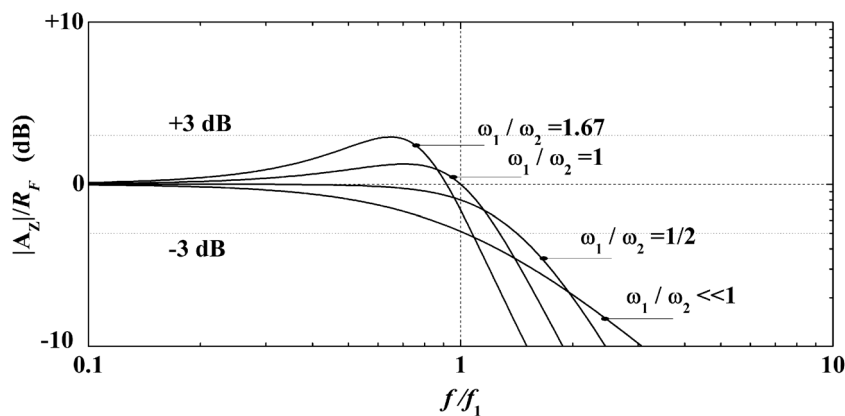


Figure 2. Normalized frequency response of the conventional transimpedance amplifier (Figure 1) for different values of the ratio between the pole frequencies of the loop gain.

$$V_{N,OUT}(s) = \left\{ I_{N,DUT} A_Z^{VSC}(s) + \left[(I_{N,OP} + I_{N,RF}) A_Z^{VSC}(s) + E_{N,OP} H_{EN,OP}^{VSC}(s) \right] \right\} H_L(s)$$

$$\begin{aligned} H_{EN,OP}^{VSC}(s) &= 1 + \frac{Z_F(s)}{Z_{IN}^N(s)} = \frac{1 + \beta_0^N(1 + \alpha_C^N)\tau_F s}{\beta_0^N(1 + \tau_F s)} \\ Z_{IN}^N(s) &= \frac{R_{DUT}}{1 + sR_{DUT}C_{IN}^N} \quad C_{IN}^N = C_{DUT} + C_{STRAY}^- + C_{CM}^- \\ \alpha_C^N &= \frac{C_{IN}^N}{C_F}; \quad \beta_0^N = \frac{R_{DUT}}{R_{DUT} + R_F} \end{aligned} \quad (12)$$

Clearly, the term into square brackets is responsible for the background noise voltage at the TIA output, that is the noise that would be present at the output with $I_{N,DUT}=0$. Using Equation (5), Equation (12) can be rewritten as:

$$V_{N,OUT}(s) = \left\{ -(I_{N,DUT} + I_{N,OP} + I_{N,RF})R_F + E_{N,OP} \left[\frac{1 + \beta_0^N(1 + \alpha_C^N)\tau_F s}{\beta_0^N} \right] \right\} \times \frac{1}{as^2 + bs + 1} \quad (13)$$

If we employ very low input noise current operational amplifiers with either MOSFET or JFET input stages, the contribution of $I_{N,OP}$ can be neglected with respect to the other sources of background noise. We can calculate the equivalent input noise spectral density $S_{IN,EQ}$ as:

$$S_{IN,EQ}(f) = \frac{S_{VN,OUT}(f)}{|A_Z(f)|^2} = S_{IN,DUT} + \frac{4kT}{R_F} + \frac{S_{EN,OP}}{(R_F\beta_0^N)^2} \left[1 + [\beta_0^N(1 + \alpha_C^N)]^2 \frac{f^2}{f_F^2} \right] \quad (14)$$

where $S_{IN,DUT}$, $S_{VN,OUT}$ and $S_{EN,OP}$ are the power spectral density associated to $I_{N,DUT}$, $V_{N,OUT}$ and $E_{N,OP}$, respectively. If we limit our analysis to cases in which f_F represents the bandwidth of the TIA, a few important conclusions can be drawn. In the first place, we observe that increasing the value of R_F decreases the contribution of the thermal noise of the feedback resistor to the background noise. However, as we have observed before, since for a given resistor technology the parasitic capacitance C_F is largely independent of R_F , increasing R_F also causes a proportional decrease in the bandwidth. Moreover, at low frequencies, the contribution of $E_{N,OP}$ is usually negligible because of the large values of R_F that are normally used in high sensitivity noise measurement applications. However, if $\alpha_C^N \gg 1$, as it is commonly the case, the contribution of $E_{N,OP}$ may become the most important contribution at frequencies well below the bandwidth limit of the system. Note that, when this occurs, the background noise is largely independent of the value of R_F and of C_F .

3. NEW TOPOLOGY FOR THE REALIZATION OF LOW-NOISE HIGH BANDWIDTH TRANSIMPEDANCE AMPLIFIER

So far we have discussed the limitations in terms of bandwidth and background noise in the conventional approach for the realization of a TIA. These limitations can be all traced back to the parasitic capacitance C_F in parallel to the feedback resistance R_F . Since the parasitic capacitance cannot be eliminated, we devised a new circuit topology for reducing, and virtually eliminating, the effect of the feedback resistance time constant on the frequency response of the amplifier. The approach that has been followed is schematized in Figure 3a. Under the virtual short circuit approximation ($|H_L(j\omega)| \approx 1$), the transimpedance gain at the output V_{OUT} is

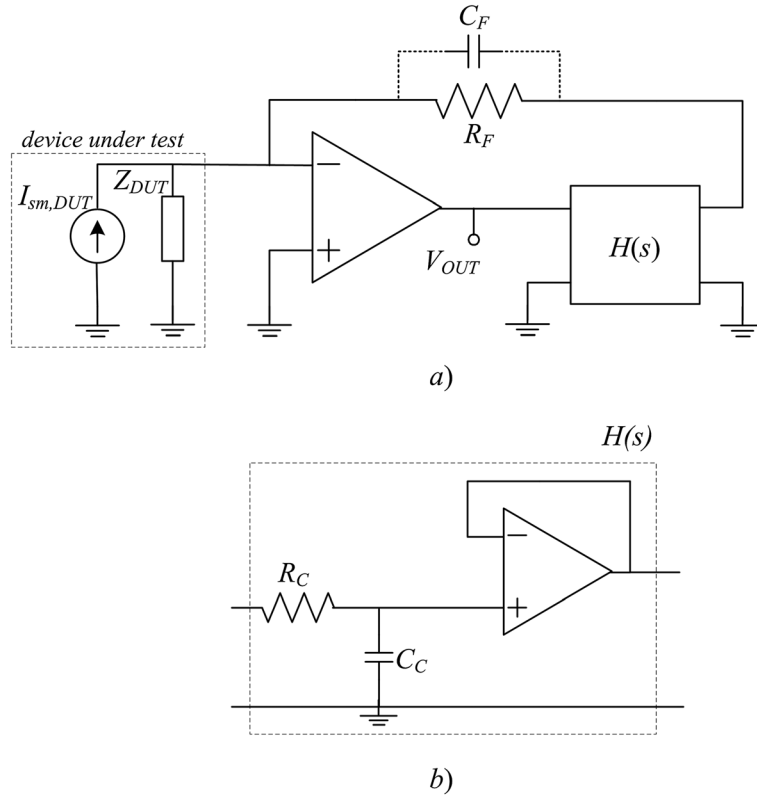


Figure 3. a) Block schematic of the proposed transimpedance amplifier; b) electrical schematic of the compensation network needed to cancel out the pole introduced by C_F .

$$A_Z^{VSC}(s) = \frac{V_{OUT}}{I_{sm,DUT}} = \frac{-R_F}{(1 + s\tau_F)H(s)} \quad (15)$$

It is therefore apparent that, with $H(s) = 1/(1 + s\tau_F)$, the effect of the parasitic capacitance C_F can be completely compensated with a flat response in the entire bandwidth into which the virtual short circuit approximation holds. Figure 3b shows the way in which the required $H(s)$ can be implemented in a quite straightforward way by means of a low pass RC circuit and a buffer with $R_C C_C = \tau_C = \tau_F$. The introduction of a low pass block in the loop gain, however, has the effect of reducing the loop gain close and above the corner frequency $f_F = 1/2\pi\tau_F$. Therefore, we can only obtain an increase in the actual bandwidth of the system, with respect to the conventional approach, if we are capable of maintaining a high value of the loop gain for frequencies much larger than f_F . We will discuss this aspect in detail in the next subsection.

3.1. Bandwidth analysis of the proposed TIA

Following the very same approach used in Section II, the expression of the actual transimpedance gain is obtained by the product of the gain in the virtual short circuit approximation (Equation (15), in this case $A_Z^{VSC} = -R_F$, independent of the frequency) by the function $H_L(s)$ that can be obtained starting from the expression of the loop gain $T(s)$ in the circuit in Figure 3a. We will assume the condition $\tau_C = \tau_F$ to be exactly verified and that the voltage follower has a bandwidth much larger than any frequency we may be interested in. Besides, the voltage follower is not really needed when we reflect on the fact that the values of R_C and C_C , as long as their product remains equal to τ_C , can be selected in such a way that the loop gain of the system is not

significantly modified by the loading effect of the impedances Z_F and Z_{IN} which are normally very large. In this situation, we obtain:

$$T(s) = -\frac{T_0}{1+s\tau_{OP}} \times \frac{1}{1+\beta_0(1+\alpha_C)s\tau_F} \quad (16)$$

and, with the same approximation as before ($A_{V0} > 1$, $T_0 > 1$) we have:

$$\begin{aligned} H_L(s) &\approx \frac{1}{as^2 + bs + 1} \\ a &\approx \frac{\tau_{OP}\tau_F(1+\alpha_C)}{A_{V0}}; \quad b = \frac{\tau_{OP}}{T_0} + \frac{1+\alpha_C}{A_{V0}}\tau_F \end{aligned} \quad (17)$$

As it can be noted, the transimpedance gain in the new approach has the very same form as in the conventional approach but with an important difference, consisting in the fact that while the term a in Equation (5) and Equation (17) are the same, the term b in Equation (17) is much smaller than the term b in Equation (5), since the dominant contribution τ_F is no longer present. We had observed that in the situation in which the term b could be assumed to be equal to τ_F , the first pole in the frequency response was indeed at or close to f_F . With a much smaller value of b (with the same value of a), we can therefore potentially obtain a larger bandwidth.

The problem with this approach, however, is that if the gain amplifier is the same operational amplifier used in the conventional approach, the transimpedance gain is characterized by complex conjugate poles with a large overshoot in the frequency response in almost any situation of interest. To understand this fact, let us take into consideration the loop gain in Equation (16). It can be easily shown that the term $H_L(s)$ can be expressed in terms of the angular frequencies ω_{OP} and ω_{FC} corresponding to the poles of $T(s)$, as follows:

$$\begin{aligned} H_L(s) &= \frac{1}{\frac{s^2}{\omega_0^2} + \frac{s}{\omega_0 Q} + 1} \\ \omega_0 &= \sqrt{A_{V0}\omega_{OP}\omega_{FC}} \quad Q = \frac{\omega_0}{\omega_{OP} + \omega_{FC}/\beta_0} \\ \omega_{FC} &= 2\pi f_{FC} = \frac{1}{(1+\alpha_C)\tau_F} \quad ; \quad \omega_{OP} = 2\pi f_{OP} = \frac{1}{\tau_{OP}} \end{aligned} \quad (18)$$

In many situations, as we have already observed, $f_{OP} \ll f_{FC}/\beta_0$, resulting in:

$$Q \approx \beta_0 \sqrt{\frac{A_{V0}f_{OP}}{f_{FC}}} = \beta_0 \sqrt{\frac{GBW}{f_{FC}}} \quad (19)$$

This means that if the pole frequency f_{FC} (which, from Equation (18), is a fraction of f_F) is much lower than the GBW of the employed operational amplifier, Q can be very large resulting in complex conjugate poles with a large overshoot in the frequency response at ω_0 . Note that for increasing DUT capacitances (that is for increasing α_C) Q increases. Since f_{FC} mainly depends on the feedback resistance and on the DUT, the only way to obtain values of Q leading to moderate overshoot or real poles is to act on the characteristics of the gain amplifier (the OA in Figure 3a). In particular, suppose we substitute the OA in Figure 3a with a more general voltage amplifier with DC gain A_{V0} and a single pole at f_{OP} with $f_{OP} > f_{FC}/\beta_0$. In this case, we would obtain:

$$Q \approx \sqrt{\frac{A_{V0}f_{FC}}{f_{OP}}} \quad (20)$$

which means that by a proper choice of A_{V0} and of the pole frequency f_{OP} we can obtain low values for Q and, assuming $Q \ll 1$, we can obtain an overall TIA bandwidth limit f_{BWL} in the order of

$$f_{BWL} \approx \frac{1}{2\pi} \omega_0 Q \approx \sqrt{A_{V0} f_{FC} f_{OP}} \times \sqrt{\frac{A_{V0} f_{FC}}{f_{OP}}} = A_{V0} f_{FC} = \frac{A_{V0}}{1 + \alpha_C} f_F \quad (21)$$

Therefore, provided that all the conditions listed above are met, we can obtain a bandwidth significantly larger than f_F (that is larger than the one in the conventional design for the same feedback resistance and DUT) if we are capable of designing the system with a voltage amplifier characterized by:

$$\begin{aligned} f_{BWL} &>> f_F \Rightarrow A_{V0} = k_A(1 + \alpha_C) \quad \text{with } k_A >> 1 \\ Q << 1 &\Rightarrow f_{OP} = k_F^2 A_{V0} f_{FC} = k_F A_{V0} \frac{f_F}{1 + \alpha_C} \quad \text{with } k_F >> 1 \end{aligned} \quad (22)$$

From the previous conditions, it follows, for the minimum gain-bandwidth product of the voltage amplifier in Figure 3a:

$$A_{V0} f_{OP} = k_A^2 k_F^2 (1 + \alpha_C) f_F \quad (23)$$

With f_F in the order of 300 Hz ($R_F = 1 \text{ G}\Omega$ and $C_F = 0.5 \text{ pF}$ as in the example before) and with α_C in the order of 20 (corresponding to C_{IN} in the order of 10 pF) and even assuming $k_A = k_F = 10$ (k_A and k_F should actually be much larger for insuring good accuracy in the conclusions drawn so far), we end up with a GBW in the order of 60 MHz, which cannot be obtained by resorting to any single low-noise, low input current operational amplifier available on the market.

In order to meet the requirements in terms of gain and bandwidth together with very low equivalent input noise sources, we can substitute the operational amplifier in Figure 3a with the cascade of $n > 1$ voltage amplifiers, the first $n - 1$ being non-inverting amplifiers and the last one being an inverting amplifier. Figure 4a shows the case $n = 2$, while Figure 4b shows all relevant noise sources and layout parasitic capacitances which are due to the first stage in Figure 4a. The response of each amplifier of the chain is characterized by a pole at the frequency $f_{PAi} = GBW_{OPi}/A_i$ ($i = 1, 2$) where GBW_{OPi} and A_i are the gain-bandwidth product and the voltage gain of the amplifier i , respectively.

Even with low values of the gain for each amplifier, a condition needed for obtaining a large bandwidth for each one of them, the overall modulus of the gain can still be quite large as it equals the product $\left| \prod_{i=1}^n A_i \right|$. The problem with this approach, however, is that we introduce $n - 1$ more poles in the loop gain, and the loop gain in Equation (16) becomes:

$$\begin{aligned} T(s) &= \prod_{i=1}^n \frac{A_i}{(1 + s\tau_{PAi})} \times \frac{\beta_0}{1 + \beta_0(1 + \alpha_C)s\tau_F} \\ \alpha_C &= (C_{DUT} + C_{STRAY}^- + C_{CM1}^+)/C_F \end{aligned} \quad (24)$$

with $\tau_{PAi} = 1/(2\pi f_{PAi})$, C_{CM1}^+ is the common mode capacitance of the not inverting input of OP₁ (not shown in Figure 4b), and the VSC has been assumed at the input of OP₁ so that the input impedance of the two-stage voltage amplifier is assumed infinite. With $n + 1$ poles in the loop gain,

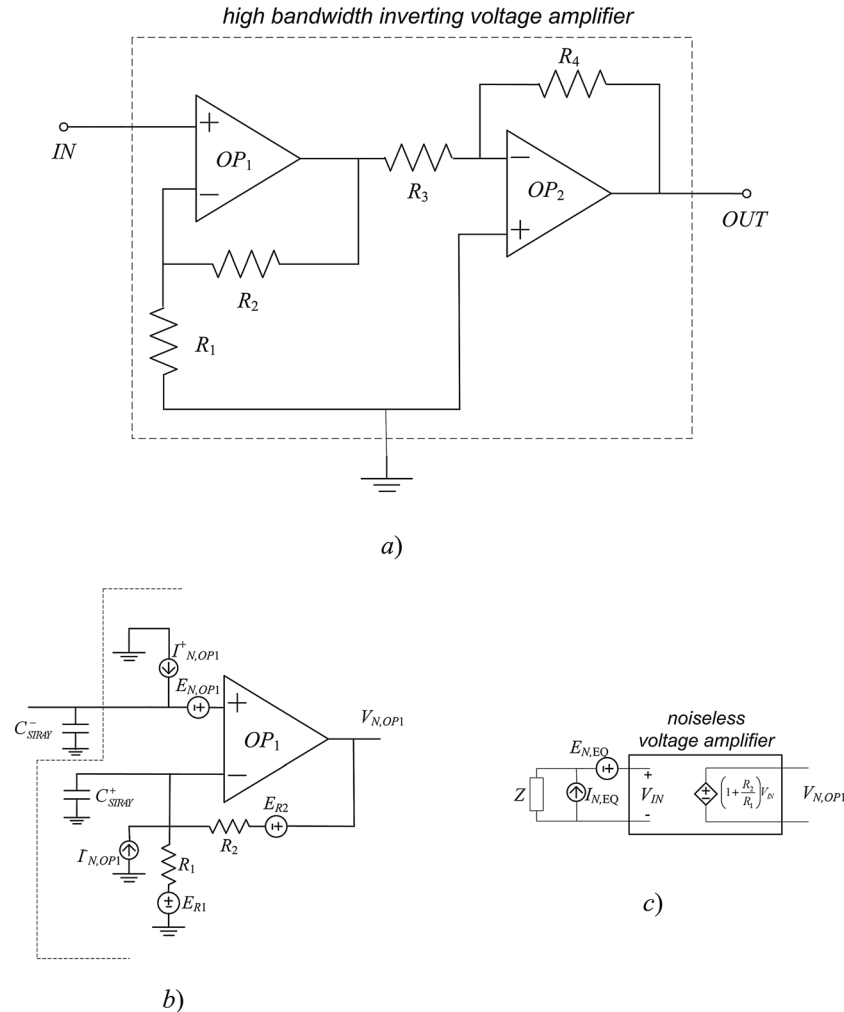


Figure 4. a) Electrical schematic of the high bandwidth inverting voltage amplifier (to be used in replacement of the opamp in Figure 3a); b) equivalent circuit for noise calculation in the first stage of the circuit in a; c) general noise model for a two-port voltage amplifier with the equivalent DUT impedance connected at the input port.

the amplifier can be prone to instability unless a proper phase margin is insured. If $n=2$, a positive phase margin is indeed obtained if the following conditions are satisfied:

$$f_{PA1}, f_{PA2} > \left| \prod_{i=1}^2 A_i \right| \frac{f_F}{(1 + \alpha_C)} \quad (25)$$

This condition corresponds to the requirement that the asymptotic amplitude bode diagram of the loop gain reaches 0 dB at a frequency below f_{PAi} . Note that the worst condition (largest required value for f_{PAi}) is obtained for $\alpha_C=0$. A value of $\alpha_C=0$ is, however, unrealistic since, even with no contribution from the DUT, $\alpha_C>0$ due to the intrinsic parasitic capacitance of OP1 (C_{CM1}^+ in Equation (24)). The condition in Equation (25) is still valid for $n>2$ if the symbol $>$ is substituted with $>>$. In this latter case ($>>$), for every n , it can be easily proven that the RHS of Equation (25) coincides with the bandwidth f_{BW} of the system. That is:

$$\text{if } f_{PAi} >> \left| \prod_{i=1}^n A_i \right| \frac{f_F}{(1 + \alpha_C)} \quad i \in [1, n] \rightarrow \quad f_{BW} = \left| \prod_{i=1}^n A_i \right| \frac{f_F}{(1 + \alpha_C)} \quad (26)$$

Equation (26) sets a limit to the maximum gain of each stage

$$f_{PAi} \approx \frac{GBW_{OPi}}{A_i} >> f_{BW} \rightarrow A_i << \frac{GBW_{OPi}}{f_{BW}} \quad (27)$$

3.2. Noise analysis of the proposed TIA

If the conditions for insuring stability in the proposed circuit are verified, we can analyze the noise performances of the proposed circuit within the bandwidth set by Equation (26) by assuming constant gains for the amplifiers stages in Figure 4a. Due to the fact that neither of the two inputs of the first stage operational amplifier is connected to ground, the noise analysis is somewhat more complicated as before. In order to simplify the analysis, we will assume that, because of the relatively large gain of the first stage, we can neglect the noise contribution of the second stage. We will therefore proceed by deriving the equivalent input voltage and current noise sources of the two port in the inset in Figure 4b according to the general model in Figure 4c. All parasitics outside the dashed line in Figure 4b can be assumed as part of the generic input impedance Z in Figure 4c. In the assumption of VSC at the input of the operational amplifier in Figure 4b, the transfer function from each noise source to the output $V_{N,OP1}$ can be obtained, as before, by assuming that each noise source is replaced by a deterministic source. We will also make the assumption, which can be easily verified, that the resistance R_1 be so small (its value in the actual circuit is 100Ω) that to all purposes we can neglect the presence of the capacitance C_{STRAY}^+ (in the order of a few pF) at all the frequencies we are interested in. We obtain:

$$V_{N,OP1} = I_{N,OP1}^+ Z \left(1 + \frac{R_2}{R_1} \right) - E_{R1} \frac{R_2}{R_1} + E_{R2} - I_{N,OP1}^- R_2 + \left(1 + \frac{R_2}{R_1} \right) E_{N,OP1} \quad (28)$$

If we perform the same calculation with reference to the equivalent circuit in Figure 4c, we obtain:

$$V_{N,OP1} = (I_{N,EQ} Z + E_{N,EQ}) \left(1 + \frac{R_2}{R_1} \right) \quad (29)$$

For Equation (28) and (29) to be equivalent for all possible Z , and assuming $R_2/R_1 >> 1$, we obtain:

$$\begin{aligned} I_{N,EQ} &= I_{N,OP1}^+ \\ E_{N,EQ} &= -E_{R1} + E_{R2} \frac{R_1}{R_2} - I_{N,OP1}^- R_1 + E_{N,OP1} \end{aligned} \quad (30)$$

The following observation can be used in order to simplify calculations:

- if R_1 is in the order of one hundred ohms and R_2/R_1 is much larger than 1, the effect of terms E_1 and E_2 , representing the thermal noise of the resistance R_1 and R_2 , respectively, can be neglected with respect to the effect of $E_{N,OP1}$. Indeed, in terms of power spectral density, the power spectral density $S_{EN,OP1}$ of $E_{N,OP1}$ of common low-voltage noise operational amplifiers is in the order of $10^{-17}\text{V}^2/\text{Hz}$ at 1 kHz, while for the power spectral densities S_{E1} and S_{E2} of E_1 and E_2 we have, for $R_1 = 100\Omega$ and $R_2/R_1 > > 1$:

$$\begin{aligned} S_{E1} &= 4kTR_1 = 1.66 \times 10^{-18}\text{V}^2/\text{Hz} << S_{EN,OP1} \\ S_{E2} &= 4kTR_2 \Rightarrow S_{E2} \left(\frac{R_1}{R_2} \right)^2 = S_{E1} \frac{R_1}{R_2} << S_{E1} << S_{EN,OP1} \end{aligned} \quad (31)$$

- since we are using very low-noise input current operational amplifiers, with R_I in the order of one hundred ohms, also the effect of the term $I_{N,OPI}R_1$ can be neglected with respect to $S_{EN,OPI}$.

Because of the observations above, therefore, we can safely assume $E_{N,EQ} \approx E_{N,OPI}$ as in the case in which a single operational amplifier was used instead of the system in Figure 4a.

Therefore, in conclusion, as far as the noise analysis of the proposed TIA is concerned, we can assume that the cascade of the two amplifier in Figure 4a is characterized by equivalent input noise and current sources essentially coincident with those at the input of the operational amplifier at the first stage. It is clear that, in this situation, the general results discussed in section II C still hold, providing the following definition is given for the parameter α_C^N

$$\alpha_C^N = (C_{DUT} + C_{STRAY}^- + C_{CM1}^+)/C_F \quad (32)$$

Indeed, if we assume, for the sake of this argument, the output of the system to be the output of the $H(j\omega)$ filter, we can regard the system as equivalent to the conventional TIA save that we are now employing an amplifier stage characterized by a very large GBW product, the only difference being in the fact that the equivalent input impedance of the cascaded amplifier chain reduces to the capacitance C_{CM1}^+ at the non inverting input of the first operational amplifier since, in the frequency range in which the VSC approximation holds, because of the shunt-series connection, the effect of the differential input impedance of the OA can be neglected. With this considerations in mind, Equation (14) still represents the total equivalent input noise at the input of the modified TIA with the important difference that it holds for frequencies that can be much larger than f_F (up to about f_{BW}). Since the background noise contribution due to the equivalent input noise voltage of the amplifier is proportional to f^2 , it is apparent that, for large values of α_C^N and/or at high frequencies, the signal-to-noise ratio decreases, and this effect, which is common to other approaches for increasing the bandwidth in similar circumstances [17, 18], cannot be corrected by acting on the loop gain of the amplifier. In these cases, and for a given feedback resistor type (with a given time constant τ_F), the value of the equivalent input voltage noise power spectrum of the amplifier and the value of α_C^N become the limiting factors.

4. EXPERIMENTAL VALIDATION

A prototype of a TIA that exploits the approach we have discussed in the previous section for the case $n=2$ has been designed, built and tested. The component list used in the circuit in Figure 5 is reported in Table I. The high GBW inverting amplifier is obtained as in Figure 4a cascading a non inverting stage and an inverting stage. The operational amplifier of the first stage is the device TLC070 which exhibits a good trade-off between GBW_{OPI} (10 MHz), C_{CM1}^+ (11 pF) and the current noise (0.6 fA/ \sqrt{Hz} at 1 kHz) to maximize the bandwidth and minimize the background noise. Differently from the first stage op-amp, the operational amplifier of the second stage has no particular requirement in terms of input capacitance and current noise, so that a larger bandwidth op-amp can be used to maximize the system bandwidth. However, excessive voltage noise of the second stage can result to significant contribution to the equivalent input voltage noise. For this reason, we have chosen the low-voltage noise (3 nV/ \sqrt{Hz} at 1 kHz) large-bandwidth ($GBW_{OP2}=64$ MHz) operational amplifier OP37. The value of the resistance R_1 (100 Ω) and R_2 (2.49 k Ω) is such that the equivalent input voltage noise spectrum at the input of the entire amplifier reduces to the equivalent input voltage noise source of the first operational amplifier in the chain. With nominal gains A_1 and A_2 for the first and second stage of 25.9 and -500, respectively, we obtain an overall nominal gain equal to -12 950 and two poles at $f_{PA1}=GBW_{OPI}/A_1 \approx 386$ kHz and $f_{PA2}=GBW_{OP2}/A_2 \approx 128$ kHz. The feedback resistance R_F is a thick film 1-G Ω resistor at 1% (see table). As will be shown later, the extrapolated R_F parasitic capacitance is about 0.27 pF, while the extrapolated layout capacitance (C_{stray}) is about 6 pF. However, the value of the parasitic capacitance of R_F is subjected to layout and temperature-induced fluctuations. In this situation, the theoretical bandwidth (Equation (26)) is

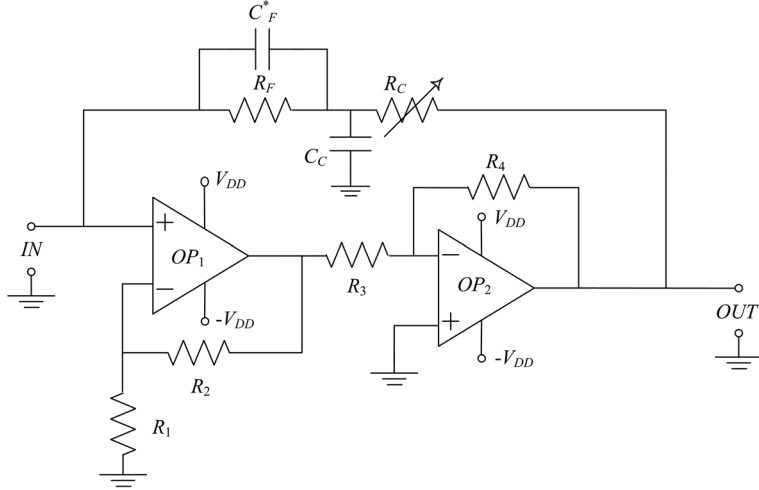


Figure 5. Electrical schematic of the proposed TIA. Actual component values are listed in Table I.

Table I. Component values used in the experimental prototype of the proposed TIA (electrical schematic in Figure 5).

Component name	Component value	Notes
R_1, R_3	100Ω	Metal film 0.1%
R_2	$2.49\text{ k}\Omega$	Metal film 0.1%
R_4	$50\text{ k}\Omega$	Metal film 0.1%
OP_1	TLC070	
OP_2	OP37	
R_F	$1\text{ G}\Omega$	HVF2512T100 Ohmite 1% Trimmer
R_C	$50\text{ k}\Omega$	
C_C	200 nF	
OP_3	TLC070	
R	$100\text{ k}\Omega$	Metal film 0.1%

therefore about 121 kHz which is not small enough with respect to both f_{PA1} and f_{PA2} to insure stability (Equation (27)). In order to address the stability/bandwidth trade-off, and to fix the total parallel capacitance to a well-known value, we added an explicit capacitor $C_F^*=3\text{ pF}$ in parallel to R_F . In this situation, the estimated theoretical bandwidth is equal to 103 kHz which results, from experiments, sufficiently lower with respect to both f_{PA1} and f_{PA2} to have stability.

The problem in measuring the performances of a TIA with such a high transimpedance gain ($1\text{ G}\Omega$) is that we require an ideal noise current source for a direct measurement of the bandwidth of the system. An actual noise source that can satisfy there requirements can be obtained with the configuration in Figure 6a as discussed in [19]. In ideal conditions (VSC approximation), the circuit in the box in Figure 6a (high-impedance current noise source or HZCNS) sources a 0 DC current into the load and behaves as an ideal current fluctuation source toward the load. Indeed, in the VSC approximation, the power spectral density S_{IS} of the current noise sourced toward the load $I_{N,S}$, is independent of the load and can be written as:

$$S_{IS} = \frac{4kT}{R} + S_{IN,OP3} + \frac{S_{EN,OP3}}{R^2} \quad (33)$$

where $S_{IN,OP3}$ and $S_{EN,OP3}$ are the power spectral densities associated to the current noise $I_{N,OP3}$ and to the voltage noise $E_{N,OP3}$, respectively (see Figure 6b). If the operational amplifier is a JFET or MOSFET input operational amplifier, unless extremely high values of R are used, the term $S_{IN,OP3}$ can be neglected at low frequencies and, if $R > > R_{min} = S_{EN,OP3}/4kT$, the current noise level is

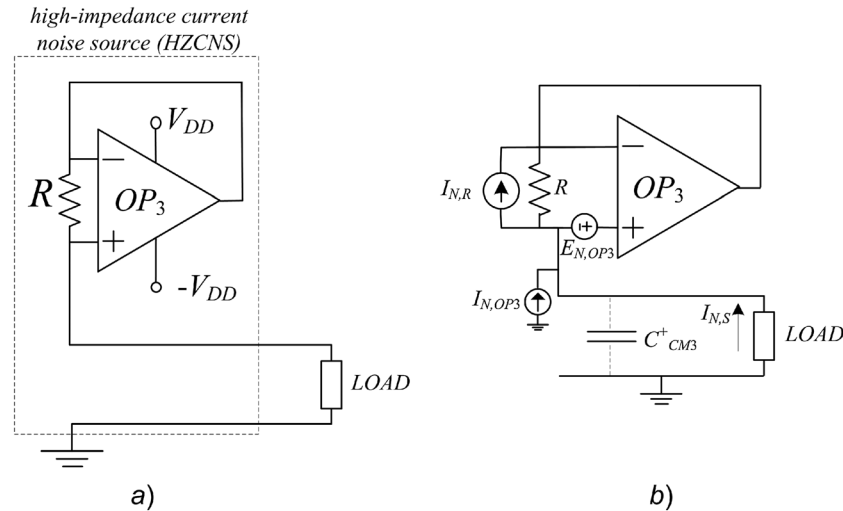


Figure 6. a) Electrical schematic of the high-impedance current noise source (HZCNS); b) equivalent circuit for noise calculation in the circuit in a).

essentially white and coincident with the thermal current noise of R . However, because $S_{IN,OP3}$ rises as f^2 , at sufficiently high frequencies it cannot be neglected, setting a maximum value to $R < R_{max} = 4kT/S_{IN,OP3}$. Therefore, by selecting a proper value of R , we can set the noise level generated by the source. As far as the output impedance is concerned, it can be easily demonstrated that at very low frequencies it can be estimated to be in the order of RA_{VO} where A_{VO} is the DC open loop voltage gain of the operational amplifier. With R in the order of a few k Ω , the low-frequency equivalent impedance of the source can reach values in the orders of hundreds of G Ω , so that, even at frequencies as low as a few Hz, the impedance of the source is actually dominated by the parasitic capacitance C_{CM3}^+ (Figure 6b) at the not inverting input of OP_3 .

Given these constraints we selected, for building the current source, the operational amplifier TLC070 which is characterized by a voltage noise equal to $7\text{nV}/\sqrt{\text{Hz}}$ at 1 kHz and current noise equal to $13\text{fA}/\sqrt{\text{Hz}}$ at 100 kHz leading to $3\text{k}\Omega = R_{min} < R < R_{max} = 100\text{M}\Omega$. Therefore, setting $R = 100\text{k}\Omega$, we obtain that the sourced noise essentially coincides with the thermal noise of the resistance ($1.67 \times 10^{-25}\text{A}^2/\text{Hz}$), that is four orders of magnitude larger than the expected TIA background noise at low frequencies ($4kT/R_F = 1.67 \times 10^{-29}\text{A}^2/\text{Hz}$). In reporting the results of the measurements that will be discussed in the following we made the choice of reporting the equivalent input noise current calculated by dividing the output voltage power spectrum by the transimpedance gain at low frequency squared. Since the input power spectrum is flat ($4kT/R$ at all investigated frequencies), we can easily obtain information on the bandwidth of the TIA from the curves obtained in this way while, at the same time, retaining the information on the noise level used for testing the response of the system.

The complete experimental setup is shown in Figure 7. The current noise source is represented as an ideal current generator with in parallel a capacitive impedance, which is due to C_{CM3}^+ as discussed above. A switch (S) allows connecting/disconnecting the source to the TIA input for bandwidth/background noise measurement respectively. An additional input capacitor (C_{DUT}) is connected at the TIA input to demonstrate the relationship between bandwidth and input capacitance (Equation (26)). The output of the TIA is recorded and elaborated by a PC-based spectrum analyzer [20] to compute spectra.

The first experiment is devoted to extract the parasitic capacitance (C_F) of 1 G Ω resistor (R_F) that is used for the feedback network of the proposed TIA. In this experiment, the switch in Figure 7 is closed, $C_{DUT}=0$, and the TIA is the conventional configuration in Figure 1a ($V_{BIAS}=0$) using the opamp TLC070. In fact, in this case the bandwidth is set by the feedback resistance time constant. This can be easily verified in Figure 8 (curve labeled ‘conventional TIA’), from which a cut-off frequency of

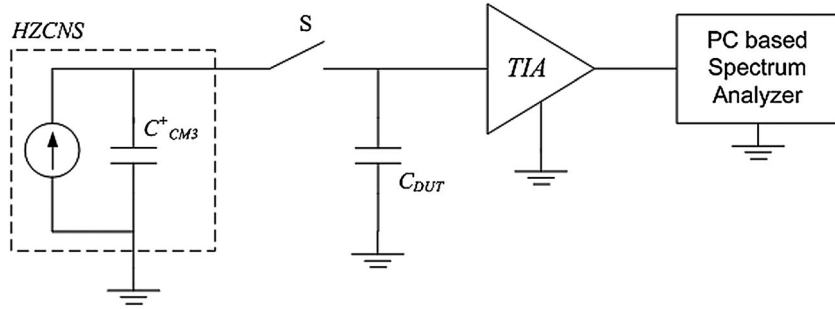


Figure 7. Experimental setup used for the measurement of the bandwidth and of the equivalent input noise of the proposed TIA.

about 590 Hz is obtained corresponding to the presence of a parasitic capacitance C_F of about 0.27 pF in parallel to the feedback resistance R_F . In the second experiment, the switch S is closed, and the TIA in Figure 7 is substituted with the proposed configuration. The knowledge of C_F allows us to preset the position of the trimmer R_C in such a way as to obtain $\tau_C = \tau_F$. Note that only if $\tau_C = \tau_F$ the frequency response will be flat near f_F . If $\tau_C < \tau_F$, then the gain for $f > f_F$ will be lower than the gain for $f < f_F$ and the converse will be true if $\tau_C > \tau_F$. This observation can be useful in that it can be used to verify by means of direct measurements that the condition $\tau_C = \tau_F$ is exactly verified and, if not, to make fine adjustments on R_C until such a condition (a flat spectrum near f_F is obtained when the white current source is at the input of the system) is exactly obtained. The result of the estimate of the input current noise (according to the approach described above) when exact frequency compensation ($\tau_C = \tau_F$) is verified is reported in Figure 8 for different values of C_{DUT} . When $C_{DUT} = 0$, the source capacitance reduces to $C_{CM3}^+ = 11$ pF. In this situation, a bandwidth of about 66 kHz is obtained (curve labeled 'proposed TIA' and $C_{DUT} = 0$ in Figure 8). The output power spectrum in this situation can be used for the estimation of the overall capacitance connected to the input of the TIA in this condition. From the fitting of this curve, we obtain an overall parasitic capacitance of about 28 pF for a value of α_C of about 104. Note that if we subtract the capacitance of the current source (11 pF), we can conclude that the total parasitic capacitance (due to both stray capacitance and the input common mode capacitance of the TLC070) is about 17 pF (11 pF can be attributed to the input TLC070 C_{CM1}^+ and 6 pF to C_{stray}). The estimated TIA bandwidth is therefore equal to about 103 kHz, a gain of more than two decades with respect to the conventional TIA (590 Hz) by using the same feedback resistance (same transimpedance gain and background noise at low frequency).

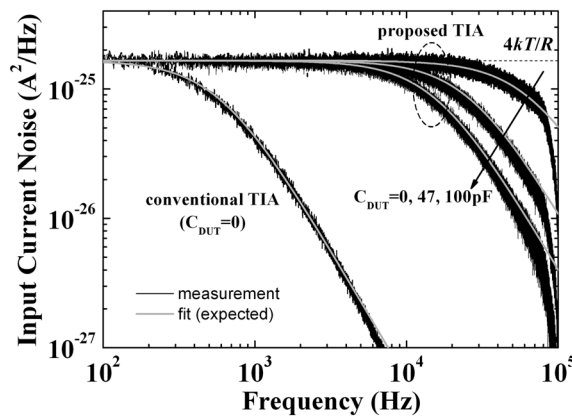


Figure 8. Measured input referred current noise spectral density of the proposed and of the conventional TIA by using the high impedance current noise source (HZCNS) as input, and for different values of a source capacitance (C_{DUT}) connected at the TIA input (black lines). The gray lines are obtained by fitting the frequency response model to the measured curves.

If we employ the extracted value for the input capacitance, we can calculate the expected frequency response when adding a capacitance (C_{DUT}) at the TIA input and compare the results with actual measurements in order to experimentally verify the analysis carried out in the previous sections. This is done in Figure 8 where the expected responses are reported together with the results of measurements with C_{DUT} set to 47 pF and 100 pF. A very good correspondence between expected curves and actual measurements is obtained. In particular, it is verified that Equation (26) does indeed provide a good estimate of the bandwidth as a function of the DUT capacitance.

The equivalent input current noise (background noise) of the TIA can be measured by simply disconnecting the current source from its input and measuring the output noise (switch S open in Figure 7). As before, we report the measurement results in the form of the output voltage noise power spectrum divided by the transimpedance gain at low frequency squared. This means that the background noise reported in Figure 9 is indeed the equivalent input noise only within the bandwidth of the amplifier. The fact that at higher frequencies the curves reported in Figure 9 appear to become flat is simply the effect of the decrease in the transimpedance gain near and above the bandwidth limit. As expected, at low frequencies, the background noise reduces to that due to the feedback resistance, while at higher frequencies the noise due to the combined effect of the equivalent input voltage noise of the amplifier and the overall capacitance (C_{DUT} and parasitic capacitances) at the input of the amplifier becomes dominant. In particular, it can be verified that increasing the input capacitance by C_{DUT} , the frequency at which the background noise rises with respect to the noise at low frequencies increases, as expected proportionally to the overall input capacitance. Because the background noise is comparable to the source noise at the bandwidth limit, the noise spectra shown in Figure 8 are free of this contribution.

5. PERFORMANCE DISCUSSION

In the previous section, we experimentally demonstrated that the proposed approach allows obtaining very large bandwidth and low noise at the same. In particular, at low frequency, the background noise corresponds to the feedback resistor current noise equal to $4fA/\sqrt{Hz}$, while a bandwidth in excess of 100 kHz has been measured. In principle, by cascading a sufficient number (n) of stages, with sufficient low gain to insure stability (Equation (27)), larger bandwidths can be obtained according to Equation (26). With respect to the conventional configuration (Figure 1a) having the same transimpedance gain and background noise at low frequency, we have found more than two orders of magnitudes in bandwidth improvement.

Other configurations have been reported that allow low noise and large in bandwidth at the same time. In [17], the pole introduced by the feedback resistor is compensated with an equal zero in a cascaded stage. In order to make a fair comparison, in Figure 10a we report an implementation of

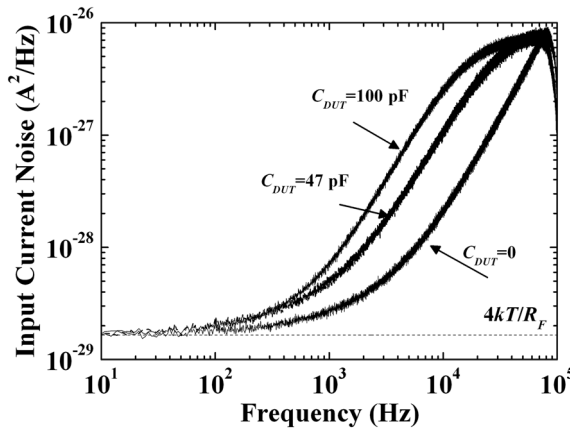


Figure 9. Measured input referred background current noise spectral density of the proposed TIA for different values of source capacitance (C_{DUT}) connected at the TIA input.

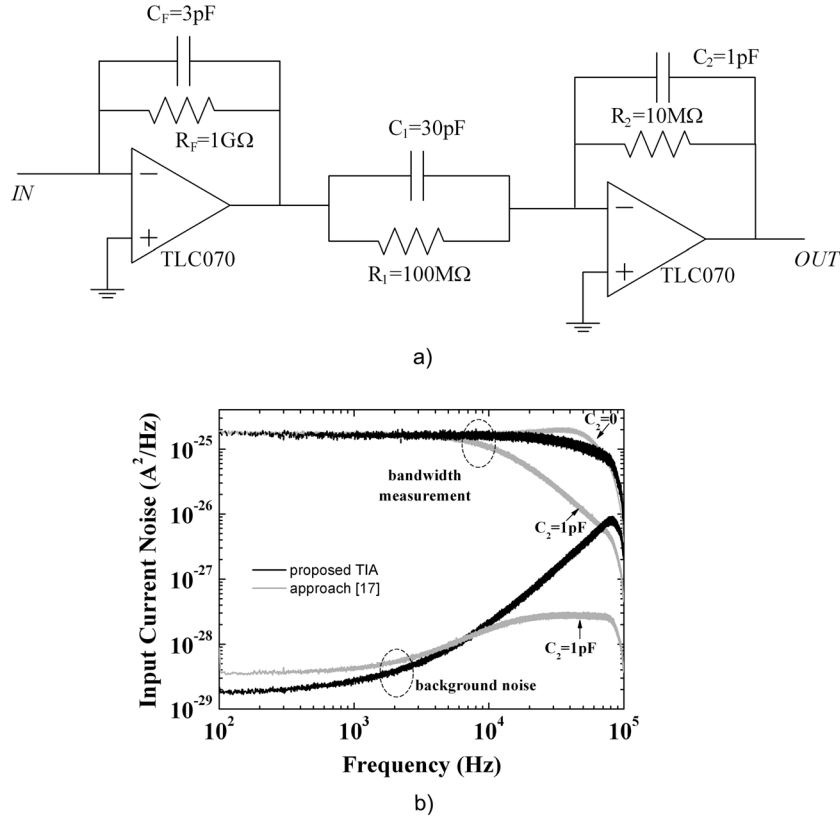


Figure 10. a) Circuital configuration proposed in [17]; b) bandwidth and background noise comparison between [17] and this work.

this approach using, in the first stage, the same op-amp and feedback impedance (same $1\text{-G}\Omega$ resistor and capacitance) as used in the realization of the proposed approach (Figure 5). In Figure 10b, the bandwidth and background noise (measured as in the previous section) of the proposed approach and those corresponding to the approach in [17] are compared. The bandwidth of in this last case is ultimately limited by the pole introduced by R_2 and its total parallel capacitance (parasitic plus external C_2). By applying the analysis of Section II, it is possible to demonstrate that, in order to ensure a one pole response within one decade, the minimum capacitance in parallel to R_2 should be about 1.3 pF . Figure 10b shows that the frequency response with no external capacitor in parallel to R_2 ($C_2 = 0$) has complex-conjugate poles, meaning that the parasitic capacitance of the resistor R_2 is not sufficient to ensure a pole dominant frequency response ($<1.3\text{ pF}$). To this purpose, we added an external $C_2 = 1\text{ pF}$ capacitor in parallel to R_2 that, together with its intrinsic parasitic capacitance, satisfies the above condition and obtained the frequency response that is shown in Figure 10b. A well-defined one pole response is indeed obtained, with an estimated 3-dB bandwidth equal to about 13 kHz . Such a bandwidth is significantly lower than the bandwidth in the prototype realized according to the new proposed approach (about 100 kHz), while, at the same time, the low-frequency noise is larger (exactly twice) due to the additional noise contribution coming from R_2 . Note that the fact that at higher frequencies, for the amplifier realized according to [17], the equivalent input noise appears to decrease with respect to the new approach is simply due to the lower bandwidth limit (see discussion in Section III B).

Figure 11 reports the time response of the proposed TIA to a square wave input. The setup measurement is reported in Figure 11a. The function generator Agilent-33220A sources a square wave at the frequency of 10 kHz with voltage levels equal to 0 V and 20 mV . The series resistor converts the input voltage to square wave current (Figure 11b left axis) with levels equal to 0 A and 2 nA . The output voltage is then recorded by the digital storage oscilloscope Agilent-DSO7052A. On the right axis in Figure 11b, it is reported that this value normalized by the transimpedance gain

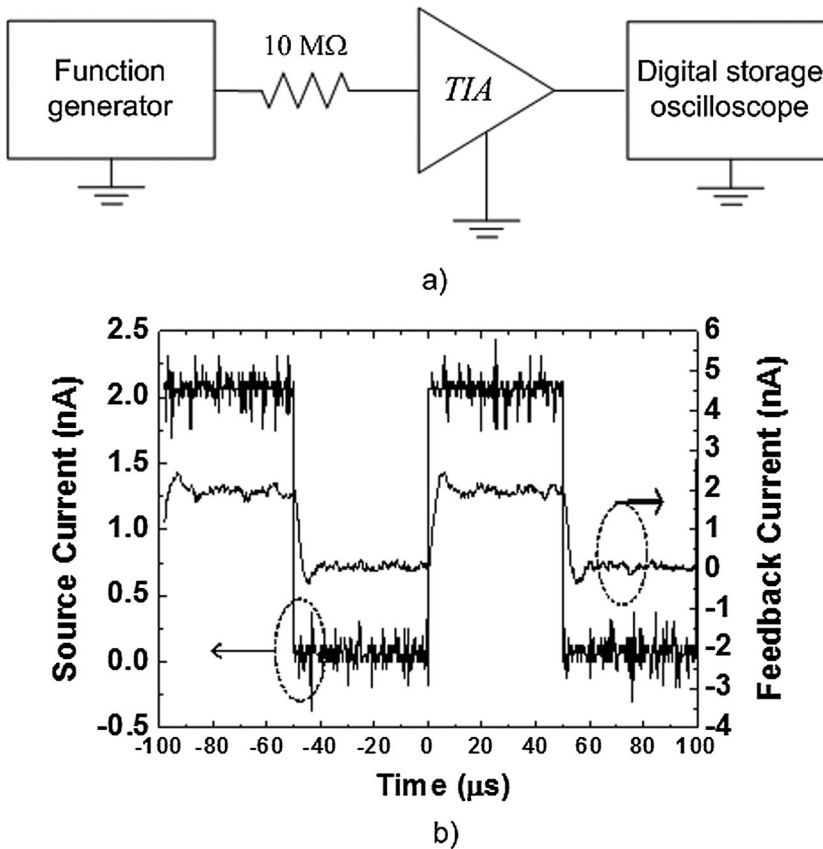


Figure 11. a) Measurement setup for signal integrity measurement; b) source and output (input referred) currents measured by means of the setup in a).

(input referred or feedback current). As it is evident from Figure 11b, the signal integrity is quite good at the output of the proposed TIA.

6. CONCLUSION

In this paper, starting from a detailed investigation of the limitations in terms of bandwidth and noise affecting the conventional topology employed for the realization of a TIA, we propose a new approach for extending the bandwidth that relies on the introduction of a proper network in the feedback loop for compensating the effect of the parasitic capacitance in parallel to the high value feedback resistor used to obtain large transimpedance gain and low noise. The conditions that need to be met for the method we propose to be effective are derived in quite general terms and can provide a clear guideline in the design of large-bandwidth TIAs in many situation of interest.

In order to prove the effectiveness of the proposed approach, we designed a prototype of a TIA with a transimpedance gain of $1\text{ G}\Omega$, a noise, at low frequencies, of about $4\text{ fA}/\sqrt{\text{Hz}}$ and a bandwidth in excess of 100 kHz . It is, however, possible, by improving the design of the inverting large GBW amplifier required for the implementation of the approach we propose, to obtain even larger bandwidths. With respect to the conventional approach, when the same type of components is employed, we obtain the same gain and the same background but with a much larger bandwidth (more than 100 kHz compared to just 590 Hz). We compared the measured performance of the proposed TIA with a previously proposed approach [17], demonstrating that the new approach can result in significantly higher bandwidth and lower low-frequency noise.

ACKNOWLEDGEMENT

This work has been funded by MIUR by means of the national Program PON R&C 2007–2013, project ‘Elettronica su Plastica per Sistemi Smart-disposable’ (PON02_00355_3416798).

REFERENCES

1. Van der Ziel A. *Noise in Solid State Devices and Circuits*. Wiley-Interscience: New York, 1986; ISBN-10: 0471832340.
2. Iqbal SM, Balasundaram G, Ghosh S, Bergstrom DE, Bashir R. Direct current electrical characterization of ds-dna in nanogap junctions. *Applied Physics Letters* 2005; **86**:153901.
3. Guan JG, Miao YQ, Zhang QJ. Impedimetric biosensors. *Journal of Bioscience and Bioengineering* 2004; **97**(4):219–226.
4. Iannaccone G, Macucci M, Pellegrini B. Shot noise in resonant-tunneling structures. *Physical Review B* 1997; **55**:4539.
5. Landauer R. Condensed-matter physics: The noise is the signal. *Nature* 1998; **392**:658–659.
6. De Jong MJM, Beenakker CWJ. Mesoscopic Electron Transport. *NATO ASI, Series E: Applied Science*. Plenum: New York, 1996.
7. Maji D, Crupi F, Giusi G, Pace C, Simoen E, Claeys C, Rao R. On the DC and Noise Properties of the Gate Current in Epitaxial Ge p-Channel Metal Oxide Semiconductor Field Effect Transistors with TiN/TaN/HfO₂/SiO₂Gate Stack. *Applied Physics Letters* 2008; **92**:163508.
8. Ciofi C, Neri B. Low-frequency noise measurements as a characterization tool for degradation phenomena in solid-state devices. *Journal of Physics D* 2000; **33**:R199.
9. Giusi G, Crupi F, Simoen E, Eneman G, Jurkzac M. Performance and Reliability of Strained Silicon nMOSFETs with SiN cap layer. *IEEE Transaction on Electron Devices* 2007; **54**(1):78–82.
10. Magnone P, Crupi F, Giusi G, Pace C, Somen E, Claeys C, Pantisano L, Maji D, Ramgopal Rao V, Srinivasan P. 1/f noise in drain and gate current of MOSFETs with high-k gate stacks. *IEEE Transactions on Device and Materials Reliability* 2009; **9**(2):180–189.
11. Giusi G, Crupi F, Ciofi C, Pace C. Instrumentation Design for Gate and Drain Low Frequency Noise Measurements. *IMTC Conf. Proc.*, Sorrento, Italy, 2006; 1747–1750.
12. (Available from: <http://www.thinksrs.com/products/SR570.htm>)
13. (Available from: <http://www.femto.de/index.html?..products/lca.html>)
14. Giusi G, Crupi F, Ciofi C, Pace C. Ultra sensitive method for current noise measurements. *Review of Scientific Instruments* 2006; **77**:015107.
15. Ciofi C, Scandurra G, Merlino R, Cannatà G, Giusi G. A New Correlation Method for High Sensitivity Current Noise Measurements. *Review of Scientific Instruments* 2007; **78**:114702.
16. Giusi G, Pace C, Crupi F. Cross-Correlation Based Trans-Impedance Amplifier for Current Noise Measurements. *International Journal of Circuit Theory and Applications* 2009; **37**(6):781–792.
17. Ciofi C, Crupi F, Pace C, Scandurra G. How to enlarge the bandwidth without increasing the noise in OP-AMP-based transimpedance amplifier. *IEEE Transactions on Instrumentation and Measurement* 2006; **55**(3).
18. Ferrari G, Sampietro M. Wide bandwidth transimpedance amplifier for extremely high sensitivity continuous measurements. *Review of Scientific Instruments* 2007; **78**:094703.
19. Giusi G, Scandurra G, Ciofi C. Large bandwidth op-amp based white noise current source. *Review of Scientific Instruments* 2014; **85**:024702.
20. Ciofi C, Giusi G, Scandurra G, Neri B. Dedicated instrumentation for high sensitive, low frequency noise measurement systems. *Fluctuation and Noise Letters* 2004; **4**(2):385–402.